

Selective Laser Sintering of Quartz Powder

Hongyun Wang, David L. Bourell, Joseph J. Beaman Jr.
Laboratory for Freedom Fabrication and Center for Materials Science and Engineering
University of Texas at Austin

Abstract

This research describes the feasibility of fusing quartz powder by Selective Laser Sintering (SLS). SLS is a method of rapid prototyping three-dimensional objects from a computer-aided design database. The effects of different processing parameters, including powder size, laser power and scan rate were explored. Single and multiple layer specimens have been made. The resulting structures were evaluated using SEM and the density of the multiple-layer structure was detected by a geometrical mass/volume technique. It was determined that particle size was the dominant variable affecting part quality. Smaller and spherical uniform particles are preferred. Future work will concentrate on optimizing powder size and shape and higher laser power.

Introduction

Preliminary experiments on SLS of quartz

Selective Laser Sintering (SLS) is a process in which a three-dimensional object is constructed directly from a computer-aided design (CAD) database without part-specific tooling or human intervention [1]. Conceived and designed at the University of Texas at Austin (UT), the process not only produces parts from polymers successfully, but is also capable of producing parts from high-temperature materials like metals and ceramics directly, without the aid of low-temperature binders. Polymers have relatively low melting temperature. They can be sintered with low laser power at relatively low operating temperatures. Ceramics melt at much higher temperatures. For example, crystalline quartz melts at 2000 K [2], making it difficult to process. Preliminary work at UT has indicated that ceramic with a polymer coating can be processed by using SLS to make turbine blade cores [3]. This present work is to test the feasibility of fusing quartz powder in an SLS apparatus and to find the optimum processing parameters for silica.

Experimental Aspects

Powder Supply

Two different kinds of powders were used. Powder A was supplied by Cyrco Quartz, Inc. Powder B was provided by the University of Texas at Austin to compare the research results.

Powder Physical Properties

Before using Powders A and B to make single or multiple layers, physical properties such as particle shape and size, surface area and crystallinity were characterized.

Particle size and shape were studied using a JSM-35C model scanning electron microscope. A Quantachrome Corporation Autosorb surface analyzer was used to measure the specific surface area of different powders, adopting the BET method. A Philips Automated Diffractometer was used to study the crystallinity and phase content of these powders.

SLS apparatus

The SLS apparatus is depicted in Figure 1.

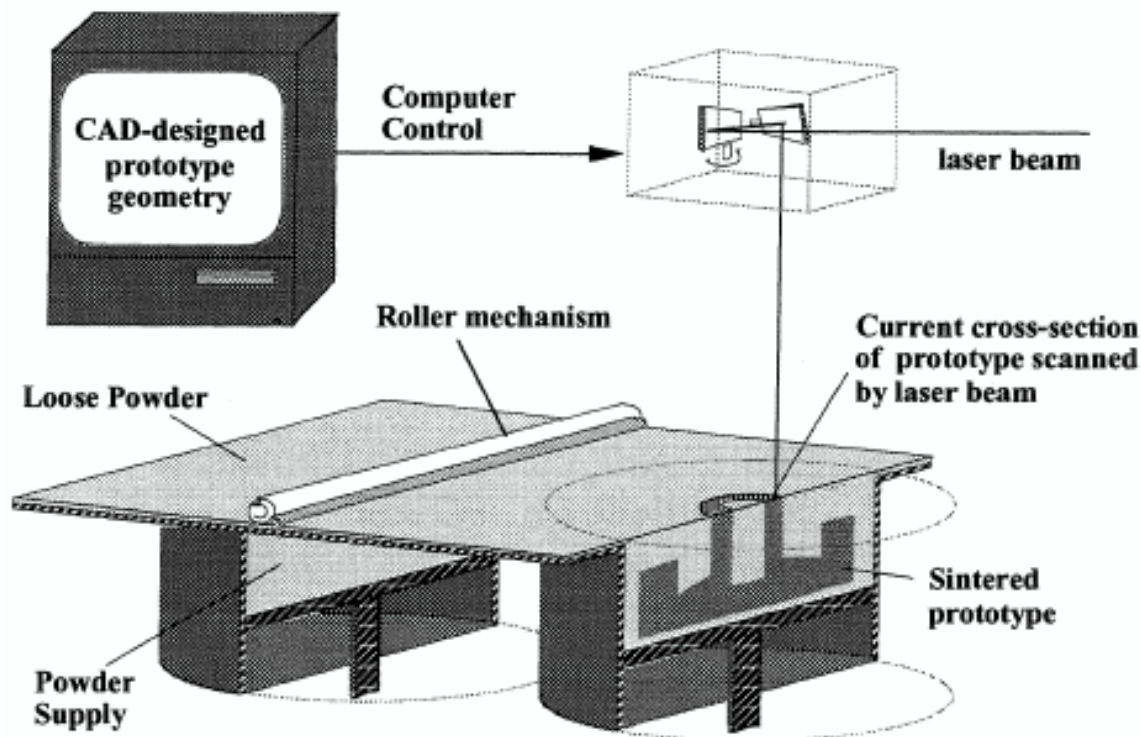


Fig. 1 A schematic drawing of an SLS process

This research was mainly performed on a UT prototype SLS machine. It has a maximum 25 watts CO_2 (wavelength = $10.6 \mu\text{m}$) laser power. The characteristic radius of the laser spot is approximately $622 \mu\text{m}$. The scanner was supplied by General Scanning Inc. Single layer structures of these powders were made. Multi-layer structures were made on a DTM beta SLS machine. For this research work, a 50 watt CO_2 laser was installed.

The microstructure, porosity and density of the specimens were studied using techniques discussed earlier for the powder.

Results and Discussion

Particle size and shape

Figure 2 shows an SEM photo of Powder A. The shape of the particle is angular and irregular. The particle size for A varied between $100 \mu\text{m}$ and $300 \mu\text{m}$. Powder B is also angular, and the particle size varied between $0.5 \mu\text{m}$ and $3 \mu\text{m}$.

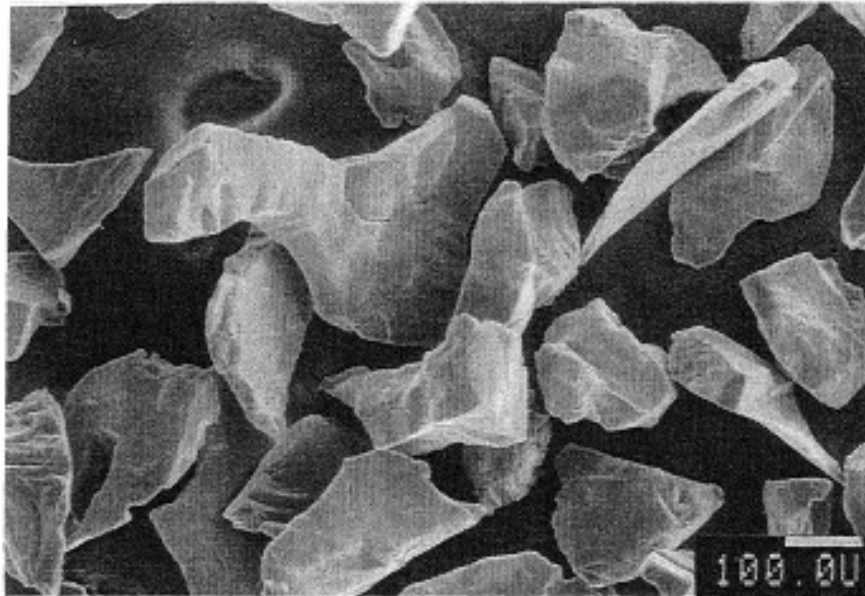


Fig. 2 SEM Photo of Powder A

X-ray analysis

From the x-ray analysis of these powders before and after laser sintering, it can be seen in Figure 3 that all powders were crystalline quartz before sintering and in Figure 4 they became amorphous silica after sintering.

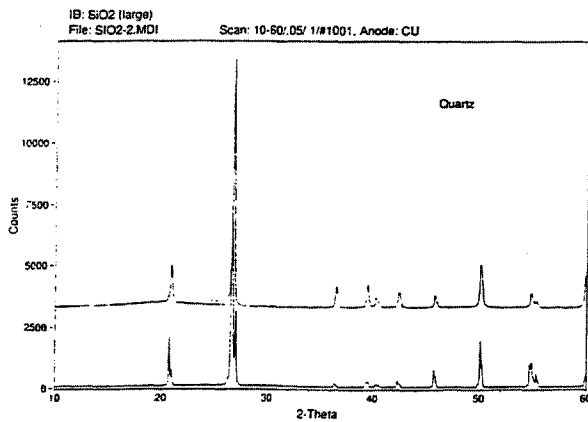


Fig. 3 XRD Pattern of Powder A and B
upper : A, lower: B; before sintering

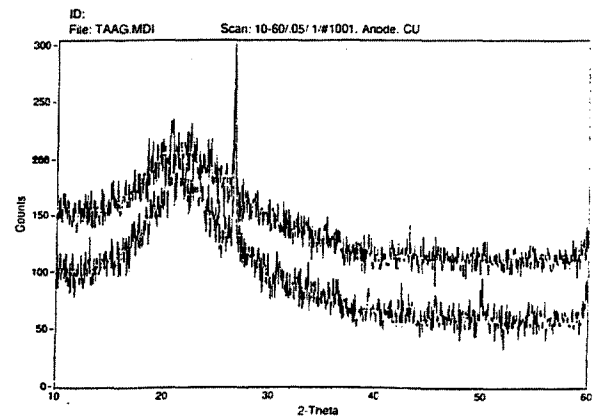


Fig. 4 XRD Pattern of Powder A and B
upper: A, lower: B; after sintering

BET results

Specific surface area plots of Powder A and B, Figure 5, confirm that smaller particles have larger surface area. The surface area of Powder A and B were $0.13 \text{ m}^2/\text{g}$ and $6.67 \text{ m}^2/\text{g}$ respectively .

Single layer runs were made on the prototype SLS machine to optimize the laser power and machine parameters, and multi-layer parts were produced on the beta SLS machine.

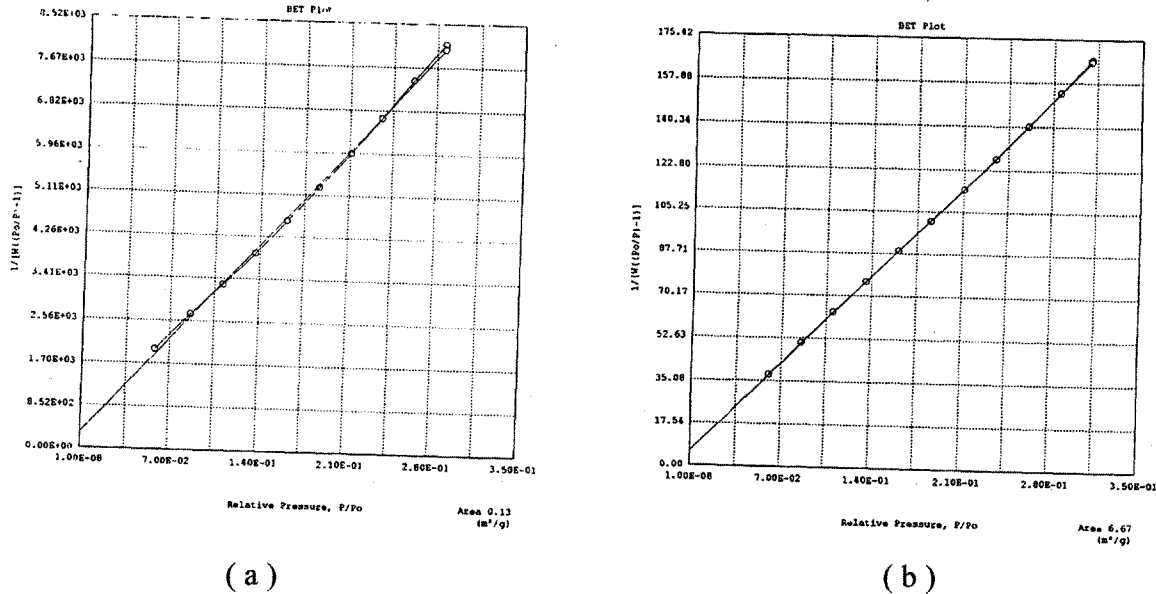


Fig. 5 BET Plots of Powder A (a) and B (b)

Single layer SLS

SLS is a process that uses a rastering laser to sinter powder particles. The laser is typically rastered at speeds from 1 to 10 cm per second. For this research, the sintering speed was about 1 to 2 cm per second. In such a short time without chemical reaction, this sintering process must involve melting to form particle necks [4]. By using identical processing parameters, single layer samples using Powders A and B were made.

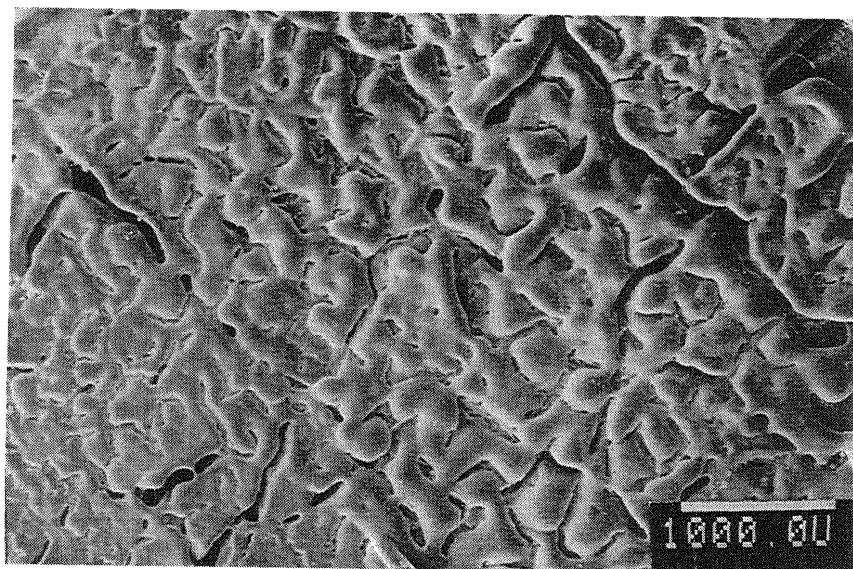
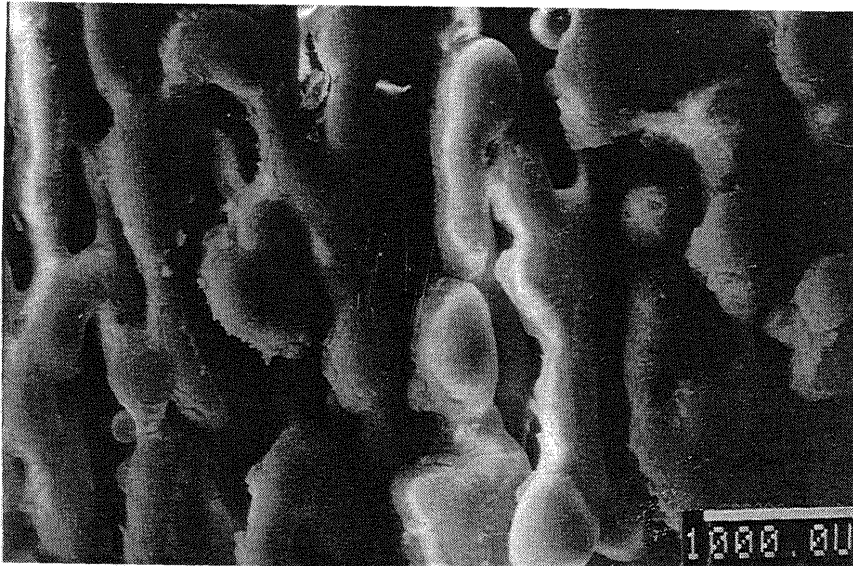
Under the same magnification, it can be seen that the lines in the SEM photo, Fig. 6a, are discontinuous, but in Fig. 6b are continuous. The characteristic radius of the laser spot is about $622 \mu\text{m}$. Because the particle shape is angular, it is difficult to compare the laser spot and particle size. This notwithstanding, the laser spot is comparable to the coarse particle size. But it is much larger than the powder particle size of Powder B. The heat conductivity of quartz powder is $0.49\text{w/m}\cdot\text{K}$ for the temperature range from 370K to 585K [5]. It is therefore difficult to conduct heat to adjacent powder particles. As a result, the volume of material in the powder bed reaching the melting point of quartz is limited to several particles directly under the moving laser beam. These areas will only experience a molten phase for a short period of time, of the order of one second. So the melting area is discontinuous for Powder A. On the other hand, the laser spot can melt a lot of Powder B at one time to form enough liquid to wet the adjacent powders and help to form continuous melting areas.

Before and after laser sintering, Powder A and B had different crystalline phases shown in Figs. 3 and 4. This is due to the rapid cooling rate associated with SLS without powder-bed heating.

The driving force for liquid phase sintering is the surface energy. The effect of surface energy is to drive the microstructure towards a minimum energy configuration by reducing the amount of free surface. Surface energy is proportional to surface area [6]. Because Powder B has larger surface area than Powder A, the driving force for Powder B is greater than Powder A. So for Powder B, the laser power is enough for liquid sintering to continue, producing the continuous lines in Fig. 6b. For the larger powder, the driving force is relatively small and the sintering

process is difficult to proceed. Additionally, laser coupling to the fine powder is better than for the coarse powder, resulting in higher local sintering temperature. To compensate for this small driving force, more laser power is needed. The limited laser power combined with the discontinuous nature of the scanning raster and low thermal conductivity is responsible for the discontinuous structure illustrated in Fig. 6a.

Particle shape also has an effect on sintering. Angular particles tend to bridge each other and cause low green packing density [7]. The low density of the powder bed is detrimental to later densification. As for the spacing between lines in Figure 6, we believe it can be eliminated by choosing appropriate sintering atmosphere and processing parameters. To get a homogeneous and continuous structure which will give high specimen density and strength, smaller and more spherical, uniform particle morphology is needed.

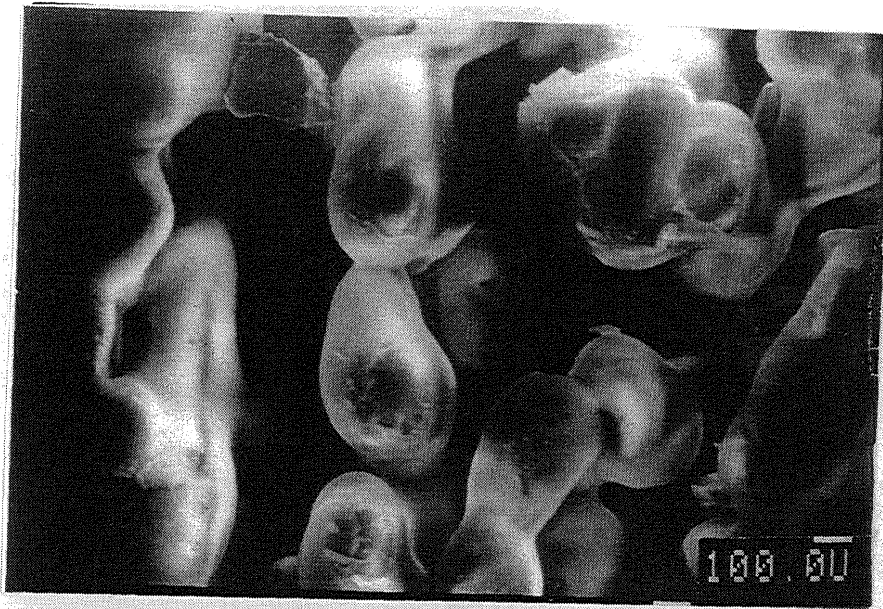


(b)

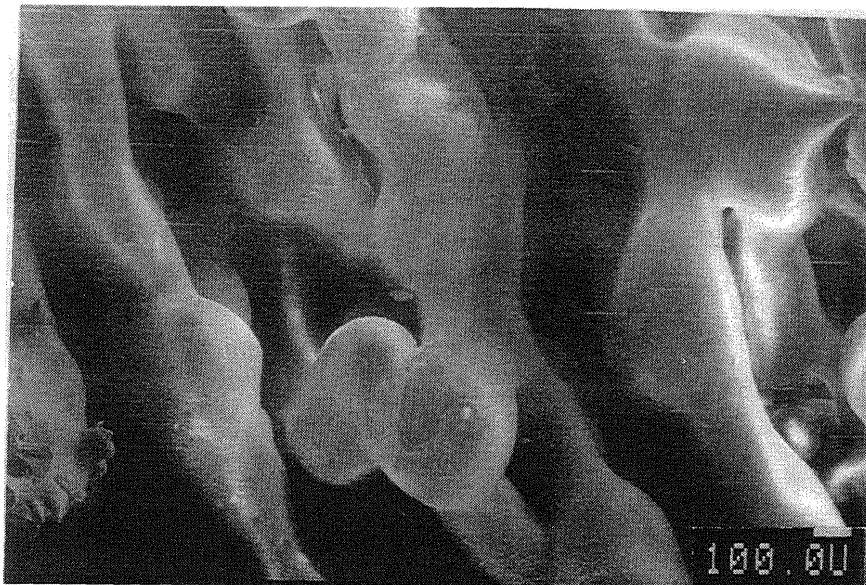
Fig. 6 SEM photos of single layer specimens made from (a) Powder A and (b) Powder B, laser power: 25 watts

Fig. 7 shows SEM photos made of Powder A by using 25 watts and 45 watts laser power, respectively. It can be seen that at 25 watts, Powder A particles only form point contacts in Fig. 7a, which means that sintering is in the initial stage of liquid sintering -- necking. Intermediate neck growth occurs at 45 watts as shown in

Fig. 7b. The point contacts formed at 25 watts laser power have formed into continuous lines at 45 watts. Higher laser power increases the degree of sintering.



(a)



(b)

Fig. 7 SEM photos of specimens made from Powder A at laser power of (a) 25 watts and (b) 45 watts

density (for quartz, the theoretical density is 2.65 g/cm^3). By using colloidal silica to infiltrate it, the parts density was increased to around 70% of theoretical density.

By using proper processing parameters and small particle size, dense structure of quartz can be made by SLS. Figure 9 shows some promising dense structures made from Powder B.

Multiple layer SLS

After the single layer tests for Powder A and B, multi-layer tests were performed. Although Powder B performed well in the single layer tests, it has higher specific surface area (Figure 5), making it difficult to spread automatically and evenly over previous layers. For optimum SLS processing, particle size should larger than $3 \mu\text{m}$. Powder A had no problem spreading. But because of its large particle, the thickness between each layer was too thick (about 3 times of the particle size which is 0.025 inch) for the laser to induce melting. By using up to 45 watts of laser power, we made several "boxes" (Figure 8) using Powder A. The laser power was still not high enough for strong interlayer bonding. By approximation, the density of these boxes is about 44% of theoretical

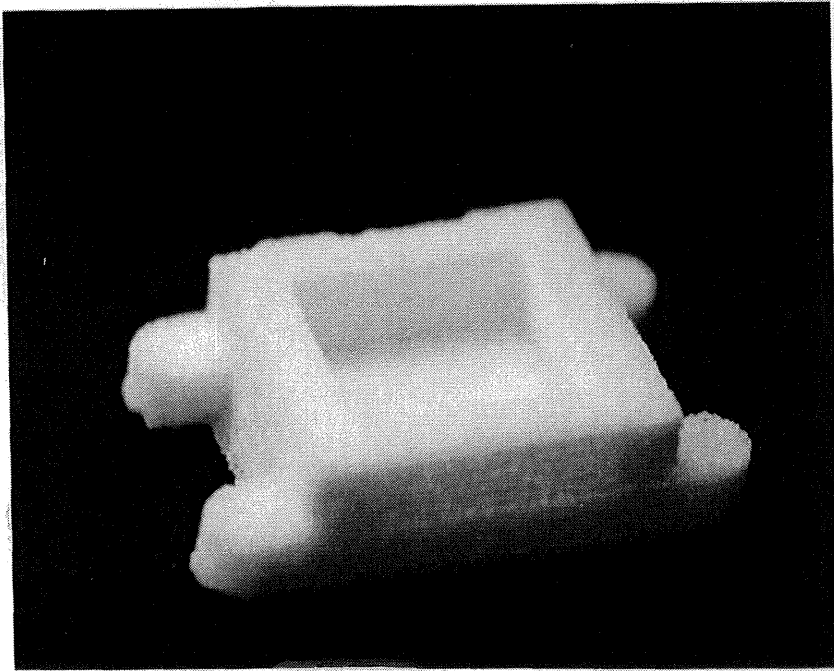
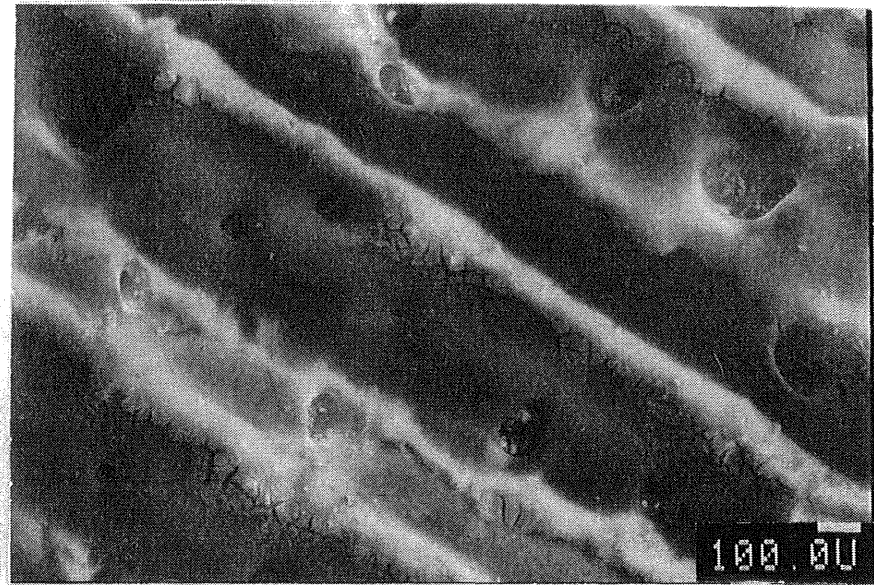
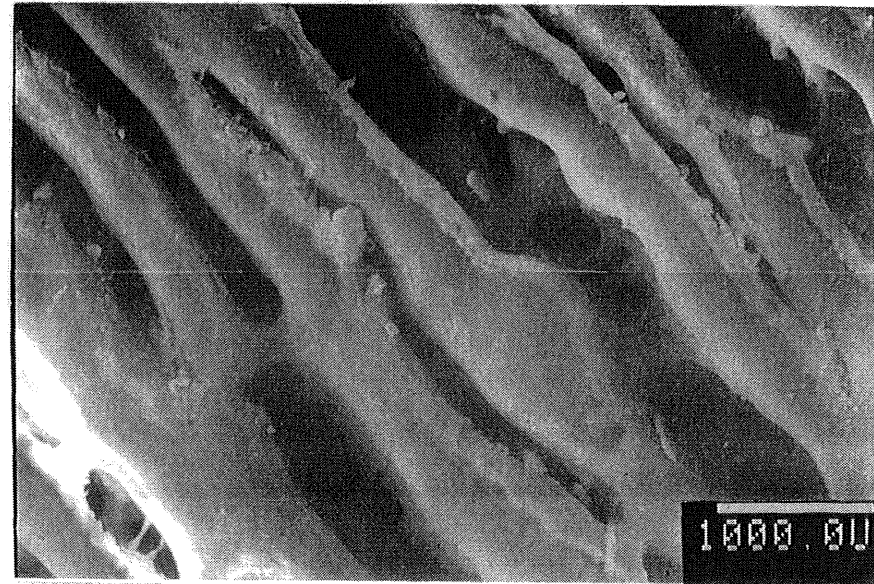


Fig. 8 Photo of multilayer box, the overall box length: 1.75 in; width: 1.25 in; height: 0.5 in.



(a)



(b)

Fig. 9 SEM photos of specimens made from Powder B, laser power 20 watts, (a) continuous scanning, (b) discontinuous scanning.

For quartz, the thermal expansion coefficients are very small, which is $14 \times 10^{-6}/^{\circ}\text{C}$ normal to the c axis and $9.0 \times 10^{-6}/^{\circ}\text{C}$ parallel to the c axis [2]. There is no significant volume change during laser sintering. This is beneficial for specimen shape design and net-shape laser fabrication processing.

Conclusions

From above work, it can be concluded that direct SLS of quartz is feasible.

Particle size and shape are very important parameter for laser sintering. The powder provided by the Cryco Inc. was too coarse and angular for optimum SLS processing. Particle size and shape not only affects the density and strength of the products, but also the appearance. Smaller spherical particles will give a smooth product surface. Powder B is too fine, an intermediate particle size is needed. From UT former work on SLS [8], typical layer thickness is controlled to lie in the 75-125 μm range. As mentioned before, layer thickness is about 3 to 4 times the particle size, so particle size around 30 to 60 μm is preferred.

Large powder sintering requires high laser power and/or slow scanning speed. Processing time is also a function of powder size and laser power. Using the same particle size, high laser power can reduce the processing time. For the multi-layer box, Fig. 8, it took approximately two hours to make at 45 watts. For higher laser power or smaller particle size, a faster scanning speed may be chosen to significantly reduce the processing time.

These initial results are very promising. Even better parts should be produceable using fine particulate and higher laser power.

Acknowledgments

The authors would like to thank Britton Birmingham, Kenwei Chen, Suman Das and Martin Wohlert for their help in this research work. The authors also acknowledge the research grants form Cryco Quartz Inc., Austin, TX.

References

1. D. L. Bourell, H. L. Marcus, J. W. Barlow, and J. J. Beaman, "Selective Laser Sintering of Metals and Ceramics", *Int. J. Powder Met.*, 28 (4), 1992
2. David W. Richerson, *Modern Ceramic Engineering*, Marcel Dekker, Inc. New York, 1992
3. James C. Nelson, Dissertation, *Selective Laser Sintering: A Definition of the Process and an Empirical Sintering Model*, The University of Texas at Austin, May 1993
4. Randall M. German, *Liquid Phase Sintering*, Plenum Press, New York, 1985
5. Y. S. Touloukian, *Thermophysical properties of Matter*, vol. 2, Plenum Press, New York, 1972
6. Randall M. German, *Sintering Theory and Practice*, New York, 1996
7. Randall M. German, *Powder Metallurgy Science*, Princeton, N. J. 1984
8. Kamatchi Subramanian, Neal Vail, Joel Barlow and Harris Marcus, "Selective Laser Sintering of Alumina with Polymer Binders", *Rapid Prototyping Journal*, vol. 1-2, 1995